A Robotic Lighting System for Solar Illumination Simulation

Richard Volpe **Douglas McAffee**
Jet Propulsion Laboratory
California Institute of Technology
Pasadena, California 91109

Abstract

This report details our development of a computer controlled spotlight with four actuated degrees-of-freedom for pan, tilt, linear movement, and beam focusing. We review the mechanical structure, kinematic model, calibration data, and control algorithm. The resultant system enables the spotlight to maintain constant intensity of the illumination of a surface, while changing the incident angle of the light. In this way, we effectively simulate the changing illumination experienced in low earth orbit. The simulation system is currently used to test human and computer inspection of orbital platform mockups for the Space Station Freedom.

1 Introduction

Later this decade, NASA will place in orbit around Earth the Space Station Freedom (SSF), which will be used as a science station and home for astronauts for 30 years. Soon after its initial design, engineering reviews revealed that simple inspection and maintenance of the station would consume more time than the astronauts would have [2]. This was reinforced by results of the Long Duration Exposure Facility (LDEF), which showed large amounts of damage from micro-meteorite and atomic oxygen degradation while in orbit for five years [6]. For these reasons, NASA sponsored *The Remote Surface Inspection Task* (RSI), a five year research project to investigate and develop ways to telerobotically inspect SSF [4].

The RSI task has three main components: manipulator control, graphical user interfacing, and automated image processing. However, these components describe parts of the inspection system, not the environment to inspected. We have also created a realistic mockup of part of the space station, complete with Orbital Replacement Units (ORUs), impact flaws, gas leaks, and temperature anomalies. This mockup is mounted on a wall next to our robot manipulator system (Robotics Research K1207 arm on a translating platform), in a room with black walls, ceiling and floor. Lighting is provided by controlled lights and flashes on the end of the arm, and by the Solar Simulation System, which is the topic of this paper.

Traditional solar simulators are designed for thermal tests of actual spacecraft [5]. To accomplish this, they utilize large vacuum chambers to house the spacecraft, and collimated lighting from arrays of xenon arc lamps. Brightness up to an order of magnitude greater than solar intensity is possible. To test the effects of changing lighting direction, the entire spacecraft is rotated while the illumination remains constant. While this approach is necessary for pre-flight spacecraft testing, it is simply not practical for robotic system prototype development.

Alternatively, we have developed a small scale simulator which effectively mimics the relative motion of the Sun in the sky, while still providing realistically scaled illumination levels. The system is composed of a spotlight mounted on a pan/tilt/translate platform. Its ability to move spatially as well as modify its beam shape, enable it to provide constant intensity illumination that changes angle of incidence at rates equal to those experienced in low earth orbit. While the simulated solar illumination is only 1.5% that of true orbital sunlight, the inspection system provides compensation by adjustment of controlled lighting position, strobe lighting pulses, and camera exposure times [1]. Therefore, the lighting conditions are a realistic test for human and machine inspection algorithms.

This paper describes the design, control, and calibration of the solar simulator, and is organized as follows. Section 2 provides a description of the electrical and mechanical components of the solar simulator system. This is followed by the description of the kinematic model of the mechanical design, including the optics of the lamp, in Section 3. Calibration of the lamp is reviewed Section 4. Section 5 discusses the control

1050-4729/94 $03.00 © 1994 IEEE

system used to ensure desired lighting trajectories. Finally, a summary and acknowledgements are provided in Sections 6 and 7.

2 Electro-Mechanical Design

Figure 1 is a photograph of the solar illumination simulation system's robotic hardware, as it appears on the ceiling of the RSI laboratory. The main component of the the simulator is a 1500 Watt xenon arc lamp. It has a cylindrical case which is about one third meter in height and diameter. The front is covered with a Fresnel lens. Inside is a translating carriage with the bulb and its reflector. The carriage is moved by turning a lead screw which protrudes through the back of the lamp, and motion of this carriage varies the beam width. The arc lamp hangs from a pan/tilt platform which translates on a linear actuator mounted to the ceiling. The axis of the tilt goes roughly through the center of mass of the lamp to reduce the necessary torque. The pan axis intersects the tilt and translation axes at right angles. Figure 2 describes the motors, encoders, and gearing employed in each of the four degrees-of-freedom (DOF).

3 Kinematic Description

3.1 Kinematic Variables

Figure 3 shows the solar illumination simulator as a five DOF system, which is represented by its state vector of configuration variables, $\boldsymbol{\theta} = (\rho, \theta, \varphi, \lambda, \gamma)$, where:

- ρ, θ, φ Spherical coordinates from the lamp center to the projected spot center.
- λ Travel of lamp from its origin frame.
- γ Lamp focus parameter indicating position of bulb carriage on internal lead screw.

These parameters have the following ranges:

	MIN	MAX
ρ	0.15 m	∞
θ	90°	180°
φ	60°	120°
λ	0	4.5 m
γ	0	0.076 m

The corresponding task state vector, $\mathbf{x} = ({}^{w}\mathbf{A}, s, \mathcal{I})$, is composed of the following variables which are also shown in Figure 3:

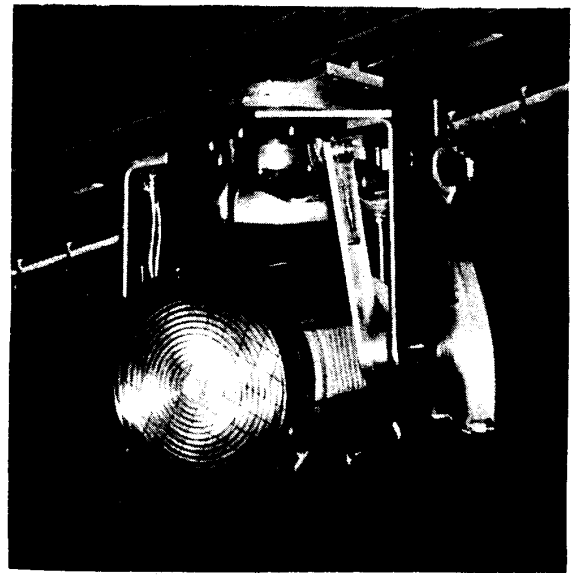

Figure 1: *A photograph of the solar illumination simulation system's robotic hardware.*

- ${}^{w}\mathbf{A}$ Cartesian vector from world frame to center of projected spot.
- s Beam angle from the lamp frame $\mathbf{n}$ axis.
- $\mathcal{I}$ Light intensity at the center of the spot on the environment.

The task vector is obtained from the configuration vector through the forward kinematics: $\mathbf{x} = \mathbf{F}(\boldsymbol{\theta})$.

Finally, it is important to note that although the kinematics has five DOF, only four are actuated. In the configuration space, the unactuated and unmeasured DOF is the radial distance from the lamp to the surface, ρ. It's value is calculated from the user specified world coordinates, ${}^{w}\mathbf{A}$. The controller is open-loop for this variable since no real-time measurement of ρ is possible.

In the task space, the unactuated and unmeasured DOF is the light intensity at the surface. Maintenance of the intensity is performed open-loop based on the calculated value of ρ and the optics model to be described.

3.2 Spatial Kinematics

The spatial kinematics govern the distances and angles as depicted in Figure 3. The transformation between the configuration and task variables is provided by the forward kinematics, $\mathbf{x} = \mathbf{F}(\boldsymbol{\theta})$:

$$x = \rho \sin\theta \cos\varphi + \lambda \quad (1)$$

$$y = \rho \sin\theta \sin\varphi \quad (2)$$

$$z = \rho \cos\theta \quad (3)$$

	Actuator 1 *Linear axis*	Actuator 2 *Yaw axis*	Actuator 3 *Pitch axis*	Actuator 4 *Bulb position*
Motor manfct	Compumotor	MicroMo	MicroMo	MicroMo
Model number	DC 3353	2842&024+23/1,66	2842&024C+23/1,246	2842&024+23/1,66:1
Output torque	80 in-oz	3 in-oz	3 in-oz	3 in-oz
Voltage	100 VDC	24 VDC	24 VDC	24 VDC
Gearhead ratio	100:1	66:1	246:1	66:1
Output torque	450 in-lbs	138 in-oz	442 in-oz	138 in-oz
Encoder manfct	Compumotor	PMI	PMI	PMI
Model No.		M1501297	M2302805	M2302805
Cnts/rev	1000	1000	1024	1024
Encoder counts / motor rev	1000	15.15	4.16	15.52
Post-encoder drive ratios	1:1	20.5:1	20:1	4.125:1
Output force	150 lbs	177 in-lbs	553 in-lbs	11 lbs
Axis motion / encoder count	0.000059 in/cnt	0.0176°/Cnt	0.0176°/Cnt	≈ 0.001in/Cnt
Encoder cnts / unit motion	267×10^6 EC/m	13050.71 EC/rad	13037.97 EC/rad	2689.08 EC/rad

Figure 2: *Description of the motors, encoders, and gearing used in the lighting system.*

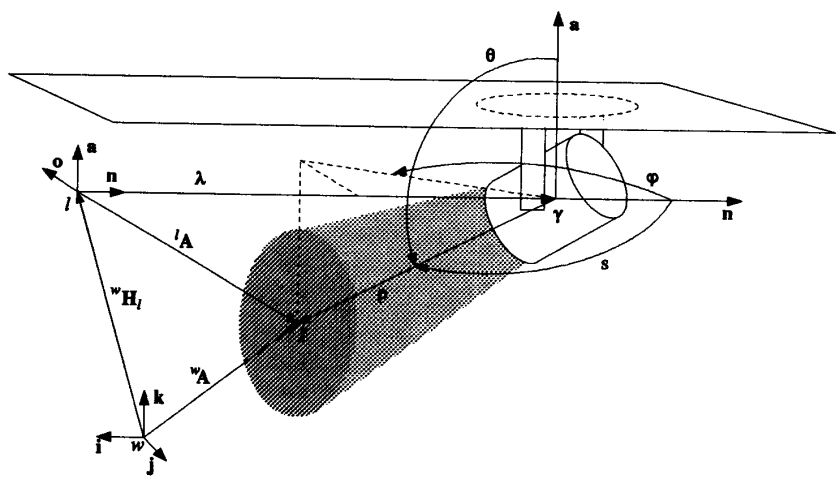

Figure 3: *The configuration and task coordinates for the solar illumination simulator system.*

$$s = \text{atan2}(\sqrt{y^2+z^2}, \lambda - x) \quad (4)$$

$$(5)$$

Where $^l\mathbf{A} = (x, y, z)$ is the vector from lamp frame origin to the illuminated spot. The lamp frame is represented by the homogeneous transform $^w\mathbf{H}_l$.

The inverse kinematics for this system, $\boldsymbol{\theta} = \mathbf{F}^{-1}(\mathbf{x})$, are given below:

$$\rho = \frac{\sqrt{y^2+z^2}}{\sin(s)} \quad (6)$$

$$\theta = \cos^{-1}\left(\frac{z}{\rho}\right) \quad (7)$$

$$\varphi = \text{atan2}(y, x - \lambda) \quad (8)$$

$$\lambda = x - \rho\cos(s) \quad (9)$$

3.3 Optical Kinematics

To project a beam of a desired intensity, it is necessary to review the optics of the lamp. Using the simple single lens model shown in Figure 4 we have the lens equation [3]:

$$\frac{1}{o} + \frac{1}{i} = \frac{1}{f} \quad (10)$$

where o, i, and f are the object, image, and focal distances. The particular case of image and object on the same side of the lens ($i < 0$) is chosen since it matches the situation with the spotlight. In this case the lamp bulb appears to be at the location of the virtual image and magnified by:

$$m = \frac{-i}{o} \quad (11)$$

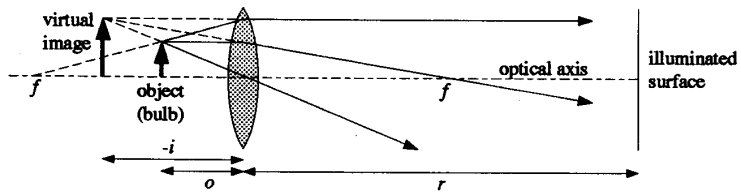

Figure 4: *The single lens optical model for the lamp.*

Assuming that the amount of light emitted by the bulb is proportional to its apparent size, and the intensity at the surface is proportional to the apparent distance, we have:

$$\mathcal{I} = C\frac{m^2}{(r+i)^2} = \frac{C}{(r+o-\frac{or}{f})^2} \tag{12}$$

where C is a constant to be determined by calibration, and r is the distance from the lamp lens to the environment. The inverse of this equation is:

$$o = \frac{\sqrt{\frac{C}{\mathcal{I}}} - r}{1 - \frac{r}{f}} \tag{13}$$

Finally, the variables r and o are related to the state variables ρ and γ by simple offsets:

$$r = \rho - \rho_o \tag{14}$$

$$o = \gamma + \gamma_o \tag{15}$$

The parameter ρ_o is the distance from the lens to the lamp center of rotation. The parameter γ_o is the distance from the lens to the most forward position of the bulb.

4 Calibration

Calibration of the lamp is needed to determine the appropriate values of the parameters C, f, ρ_o, and γ_o from the previous section. To do this, two sets of measurements were taken with a photometer. To reduce the intensity of the lamp to the measurement range of the photometer, a neutral density filter was used. The measured intensity reduction of this filter was 81%. Therefore, all plotted values were divided by 0.19 to compensate.

All optical calibration was done at the center of the projected beam. This was done so that the simplest optical model could be employed, and since the intensity distribution across the beam varied for different beam center intensities. Figures 5 and 6 show this clearly for the maximum and minimum settings of γ. The logarithmic plot in Figure 7 accentuates the off-axis intensity profile.

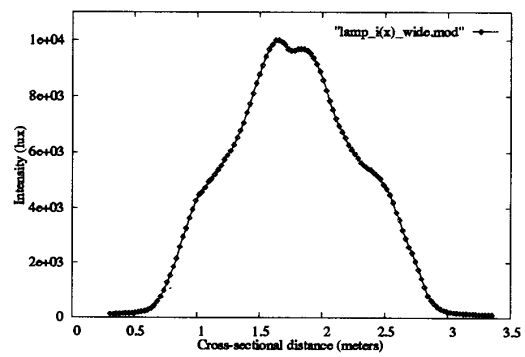

Figure 5: *Lamp intensity cross-section for foremost bulb position and $r = 2.17$ m [85.5 in].*

Using the central beam location, the relation of intensity to lamp distance was obtained by moving the photometer along the optical axis with the bulb at its foremost and aftmost positions. Figure 8 shows the measured data points and the predicted curves. The intersection of these two curves provides the focal length of the lens, $f \approx 0.18$ m [7.25 in]. The bulb offset was first measured as $\gamma_o = 0.0889$ m [3.5 in] and then adjusted to 0.0876 m [3.45 in] for a better curve fit. The necessary scaling factor to match the data was $C = 1.53 \times 10^4$ lux $\cdot$ m^2 [4.5×10^6 lux $\cdot$ in^2].

Second, the photometer was mounted at a constant distance ($r = 2.17$ m [88.5 in]) with the axes of the lamp and meter aligned. The bulb was moved from its foremost to its aftmost position in the lamp, and the intensity was measured for each setting. Figure 9 shows the measured data points, as well as the predicted curve. These accurate results provide independent confirmation of the extracted parameters. Further, it indicates the functional shape between the two curves of Figure 8. This can be more clearly seen by plotting Equation 12 as in Figure 10.

Finally, the value of $\rho \approx 0.178$ m [7 in] was determined by measuring the distance from the front lens

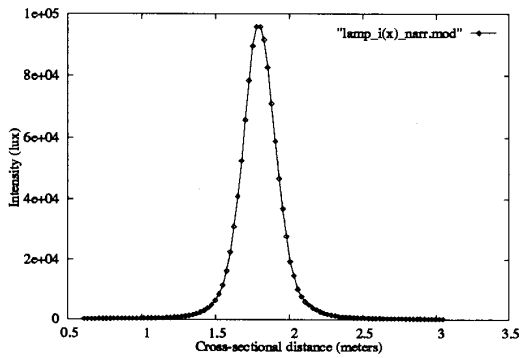

Figure 6: *Lamp intensity cross-section for aftmost bulb position and $r = 2.17$ m [85.5 in].*

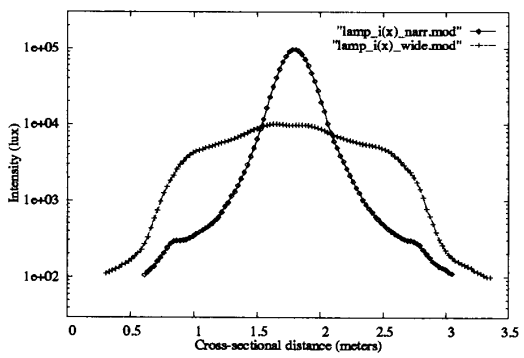

Figure 7: *Comparison of lamp intensity cross-sections for wide and narrow beams at $r = 2.17$ m [85.5 in]. Logarithmic plotting accentuates the off-axis structure.*

to the pitch axis. To confirm the measurement, the intensity at the illuminated surface was specified, and corroborated with the photometer.

5 Control

The control of the solar simulator has two levels: joint and task level.

At the joint servo level, we use Precision MicroControl's DCX VM100 programmable motor controllers. The DCX controller is a VMEbus based system, with the extensibility to control up to 6 motors at one time. Communication is accomplished across the backplane, using a driver written to emulate the serial communication protocol provided by the company.

Because the encoders are incremental, calibration

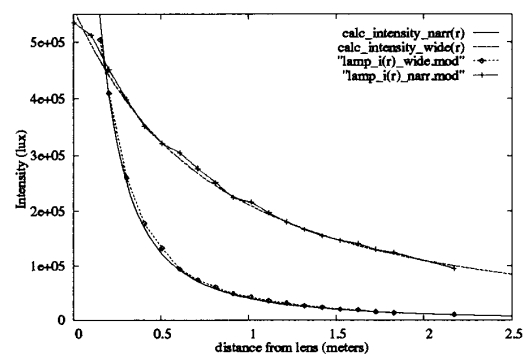

Figure 8: *Lamp intensity as a function of distance from lamp lens. Also shown are the curve fits based on the optical model.*

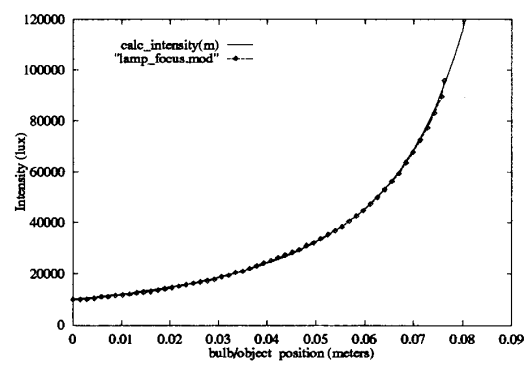

Figure 9: *Lamp intensity as a function of bulb position. The diamonds connected by a dotted line are data points, measured at 2.17 m. The solid line is a curve fit based on the optical model.*

of the solar simulator is needed each time the system is used. During calibration, position moves are commanded which are equal to the maximum change for each DOF. The DCX controller executes such position move commands with trapezoidal velocity profile trajectories, with user selectable maximum velocity and acceleration. Limit switches prevent motion beyond the stop for each DOF. Homing is then performed in the stopped (known) configuration.

When controlling the system, the same joint position move commands used for homing can not be used. This is because the trapezoidal velocity profiles for each joint will not provide coordinated task space motion. Further, the controller is designed to require stopping between all joint position motion commands. There-

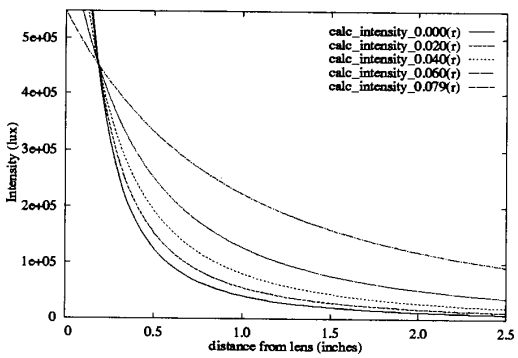

Figure 10: *Lamp intensity as a function of distance from the lamp for several bulb positions. The curve values, from bottom to top are for $\gamma = \gamma_o + o$ with $\gamma_o = 0.0889$ m [3.5 in] and o = 0, 2, 4, 6, and 7.9 cm.*

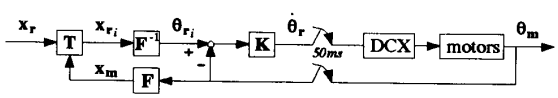

Figure 11: *Block diagram of the solar simulator controller.*

fore, continuous task space motion is only possible if the DCX controller is placed in velocity mode, and incremental joint motions are affected by commanding velocities for known time intervals.

The incremental velocities are computed in a control loop running on a separate 68020 processor, under the VxWorks operating system. Figure 11 is a block diagram of this controller. The forward kinematics, $\mathbf{F}$, are used to compute the current task variable values, $\mathbf{x}_m$, from the measured configuration variable values, $\boldsymbol{\theta}_m$. The trajectory generation program, $\mathbf{T}$, then displays the task variable values and prompts the user for new values and a time of transition, $\mathbf{x}_r$. From the old and new values, an average velocity of transition is determined. Cycling at the predetermined sampling rate, the trajectory generation routine uses a specified velocity profile (usually constant) to generate intermediate task space reference values, $\mathbf{x}_{r_i}$. These intermediate reference values are transformed to their configuration space counterparts, $\boldsymbol{\theta}_{r_i}$, through the inverse kinematics, $\mathbf{F}^{-1}$. Every sampling period, the measured configuration position values are compared against the intermediate reference configuration position values. The difference is multiplied by a gain, $\mathbf{K}$, divided by the sample time, and sent to the DCX controller as the reference velocity for that cycle. For our implementation, the sampling period was 50 ms, and the proportional gain was 10.

6 Summary

This paper has described our development of a robotic lighting system for simulating the changes in solar illumination experienced in earth orbit. The system consists of a xenon arc lamp with beam focusing, mounted on a pan/tilt/translate platform. We have described our design for this mechanical system, as well as the kinematic model and calibration data. The four DOFs have been actuated and computer controlled, allowing specification of the surface to be illuminated, the angle of illumination, and the intensity. The resulting system effectively simulates changing orbital sunlight conditions, enabling realistic testing of robotic inspection with our SSF mock-up.

7 Acknowledgments

The authors would like to thank Ray Spencer and David Lim for their help in creating this working system. The research described in this paper was carried out by the Jet Propulsion Laboratory, California Institute of Technology, under a contract with the National Aeronautics and Space Administration. Reference herein to any specific commercial product, process, or service by trade name, trademark, manufacturer, or otherwise, does not constitute or imply its endorsement by the United States Government or the Jet Propulsion Laboratory, California Institute of Technology.

References

[1] J. Balaram. Automated Visual Change Detection For Remote Surface Inspection. Internal Engineering Memorandum 3474-93-004, Jet Propulsion Laboratory, California Institute of Technology, Pasadena, CA, September 1993.

[2] F. Fisher and C Price. Space Station Freedom External Maintenance Task Team — Final Report. Technical report, Johnson Space Center, Houston, Texas, July 1990.

[3] D. Haliday and R. Resnick. *Fundamentals of Physics*. John Wiley and Sons, New York, 1981.

[4] S. Hayati et al. A Telerobotic System for Remote Surface Inspection. In *Internation Workshop on Inspection and Evaluation of Aging Aircraft*, Albuquerque, NM, May 18-21 1992.

[5] Our Captive Space: JPL Space Simulator Facilities. Brochure 400-68, Jet Propulsion Laboratory, California Institute of Technology, Pasadena, California, September 1993.

[6] T. See et al. Meteoroid and Debris Impact Features Documented on the Long Duration Exposure Facility. Technical Report 24608, Johnson Space Center, Houston, Texas, August 1990.